# Illustrative example: System data, controllers and simulation results[1]

*Online supplement to "Local Mode Dependent Decentralized Stabilization of Uncertain Markovian Jump Large-scale Systems", published on the IEEE Transactions on Automatic Control*

Junlin Xiong, Valery A. Ugrinovskii, and Ian R. Petersen

This supplement provides the system data, the gains of the designed local mode dependent controller and the comparison global mode dependent controller, and the simulation results for the illustrative example considered in the above paper. It is available online as Reference [10] of the above paper.

## A. System Data

To illustrate the control design methodology developed in the above paper, we consider a large-scale system of the form (1) governed by the Markov process introduced in Example 1 of the paper. The system consists of three subsystems; each subsystem has two modes, which are dependent, as described in Example 1 of the paper.

The system data for the system of the form (1) were generated randomly in $[-1,1]$, and are as follows:

$$A_1(1)=\begin{bmatrix}-0.9008 & -0.2983\\ -0.8238 & -0.9054\end{bmatrix},\quad A_1(2)=\begin{bmatrix}0.0423 & 0.4967\\ -0.4432 & -0.1437\end{bmatrix},\quad A_2(1)=\begin{bmatrix}0.3342 & 0.8137\\ -0.5166 & -0.4552\end{bmatrix},$$

$$A_2(2)=\begin{bmatrix}-0.6306 & 0.7007\\ -0.2009 & 0.1661\end{bmatrix},\quad A_3(1)=\begin{bmatrix}-0.3081 & 0.4407\\ -0.0742 & -0.9937\end{bmatrix},\quad A_3(2)=\begin{bmatrix}-0.6750 & 0.2201\\ -0.8136 & 0.7202\end{bmatrix},$$

$$B_1(1)=\begin{bmatrix}0.5995\\ 0.2861\end{bmatrix},\quad B_1(2)=\begin{bmatrix}0.1091\\ 0.9505\end{bmatrix},\quad B_2(1)=\begin{bmatrix}0.1500\\ -0.3223\end{bmatrix},$$

$$B_2(2)=\begin{bmatrix}-0.6282\\ -0.3214\end{bmatrix},\quad B_3(1)=\begin{bmatrix}-0.9691\\ 0.1877\end{bmatrix},\quad B_3(2)=\begin{bmatrix}0.8839\\ -0.9676\end{bmatrix},$$

[1]School of Engineering and Information Technology, University of New South Wales at the Australian Defence Force Academy, Canberra ACT 2600, Australia.

$$E_1(1)=\begin{bmatrix}0.7597\\0.9868\end{bmatrix},\qquad E_1(2)=\begin{bmatrix}-0.1505\\0.0330\end{bmatrix},\qquad E_2(1)=\begin{bmatrix}0.6275\\-0.6102\end{bmatrix},$$
$$E_2(2)=\begin{bmatrix}0.9701\\0.4312\end{bmatrix},\qquad E_3(1)=\begin{bmatrix}0.8567\\0.9628\end{bmatrix},\qquad E_3(2)=\begin{bmatrix}-0.0461\\0.8370\end{bmatrix},$$
$$L_1(1)=\begin{bmatrix}0.2988\\0.4741\end{bmatrix},\qquad L_1(2)=\begin{bmatrix}-0.2247\\-0.6858\end{bmatrix},\qquad L_2(1)=\begin{bmatrix}-0.4837\\-0.3653\end{bmatrix},$$
$$L_2(2)=\begin{bmatrix}0.7467\\0.6869\end{bmatrix},\qquad L_3(1)=\begin{bmatrix}0.8435\\-0.3380\end{bmatrix},\qquad L_3(2)=\begin{bmatrix}0.8272\\-0.8268\end{bmatrix},$$
$$H_1(1)=\begin{bmatrix}0.2623 & -0.2782\end{bmatrix},\qquad H_1(2)=\begin{bmatrix}0.0866 & 0.5032\end{bmatrix},\qquad H_2(1)=\begin{bmatrix}-0.1207 & -0.9387\end{bmatrix},$$
$$H_2(2)=\begin{bmatrix}-0.5241 & 0.1379\end{bmatrix},\qquad H_3(1)=\begin{bmatrix}0.6554 & -0.9807\end{bmatrix},\qquad H_3(2)=\begin{bmatrix}0.9278 & -0.8591\end{bmatrix}.$$

The weighting matrices in the cost functional (9) are given by

$$Q_i(\mu)=R_i(\mu)=\begin{bmatrix}0.009 & 0\\0 & 0.009\end{bmatrix},\qquad i=1,2,3,\quad \mu=1,\ldots,4.$$

Moreover, the initial condition of the system was assumed to be $x_{10}=\begin{bmatrix}5 & -5\end{bmatrix}^T$, $x_{20}=\begin{bmatrix}3 & -3\end{bmatrix}^T$, $x_{30}=\begin{bmatrix}1 & -1\end{bmatrix}^T$, $\eta_{10}=\eta_{20}=\eta_{30}=1$. The positive matrices in (2) and (3) are given by

$$\bar{S}_i=\tilde{S}_i=\begin{bmatrix}0.01 & 0\\0 & 0.01\end{bmatrix},\qquad i=1,2,3.$$

*B. Designed Controllers*

*1) Local mode dependent controller:* Solving the optimization problem stated in Section IV and following the design procedure given in Theorem 4, we obtained the gains of the local mode dependent controller of the form (4):

$$K_1(1)=\begin{bmatrix}-10.5936 & 0.9251\end{bmatrix},\qquad K_1(2)=\begin{bmatrix}-5.6461 & -15.5945\end{bmatrix},$$
$$K_2(1)=\begin{bmatrix}20.7167 & 25.0502\end{bmatrix},\qquad K_2(2)=\begin{bmatrix}20.0495 & 13.7498\end{bmatrix},$$
$$K_3(1)=\begin{bmatrix}30.9617 & -38.1042\end{bmatrix},\qquad K_3(2)=\begin{bmatrix}-54.7347 & 61.4017\end{bmatrix}.$$

Thus, the local mode dependent controller consists of a 2-gain schedule for each subsystem, 6 control gains in total.

*2) The comparison minimax optimal global mode dependent controller:* The comparison minimax optimal global mode dependent controller was obtained by solving the worst-case optimization problem stated in Theorem 2 of [5]. The gains of the optimal global mode dependent controller of the form (8) were found to be

$$K_1(1) = \begin{bmatrix} -1.8723 & 1.0433 \end{bmatrix}, \qquad K_1(2) = \begin{bmatrix} -2.7211 & -0.1547 \end{bmatrix},$$
$$K_1(3) = \begin{bmatrix} -0.8906 & -4.5858 \end{bmatrix}, \qquad K_1(4) = \begin{bmatrix} -2.0000 & -4.7295 \end{bmatrix},$$
$$K_2(1) = \begin{bmatrix} 9.7479 & 11.7835 \end{bmatrix}, \qquad K_2(2) = \begin{bmatrix} 6.1118 & 5.9448 \end{bmatrix},$$
$$K_2(3) = \begin{bmatrix} 3.2898 & 6.8148 \end{bmatrix}, \qquad K_2(4) = \begin{bmatrix} 4.8150 & 4.8724 \end{bmatrix},$$
$$K_3(1) = \begin{bmatrix} 10.3377 & -12.5929 \end{bmatrix}, \qquad K_3(2) = \begin{bmatrix} -11.9049 & 12.8609 \end{bmatrix},$$
$$K_3(3) = \begin{bmatrix} -11.7675 & 12.3645 \end{bmatrix}, \qquad K_3(4) = \begin{bmatrix} 10.2507 & -12.4495 \end{bmatrix}.$$

Thus, the comparison controller consists of a 4-gain schedule for each subsystem and involves 12 control gains in total.

### *C. Simulation results and Illustrating Figures*

Simulations were carried out to illustrate the properties of the local mode dependent controller designed using the technique proposed in this paper. The admissible local uncertainties and interconnections were chosen to have the stable linear dynamic form

$$\begin{cases} \dot{x}_{\xi i}(t) = -\alpha x_{\xi i}(t) + \alpha \zeta_i(t), \\ \xi_i(t) = x_{\xi i}(t), \end{cases} \quad \text{and} \quad \begin{cases} \dot{x}_{ri}(t) = \beta \begin{bmatrix} -1 & 1 \\ -1 & -1 \end{bmatrix} x_{ri}(t) + \beta \begin{bmatrix} 1 \\ 1 \end{bmatrix} \sum_{j=1, j\neq i}^{3} \zeta_j(t), \\ r_i(t) = \begin{bmatrix} 0.7 & -0.7 \end{bmatrix} x_{ri}(t), \end{cases}$$

where $\alpha > 0$ and $\beta > 0$ are uncertain parameters. With these particular uncertainties and the controller designed using our approach, the stability properties of the open-loop and the closed-loop large-scale systems are easy to verify by substituting the uncertainties into the system and forming a corresponding Markovian jump linear system. It is found that the open-loop system is not stochastically stable while the closed-loop system using the constructed controller was found to be robustly stochastically stable; this confirms the result of Theorem 4.

A random sample of the global mode process $\eta(t)$ was generated and used in the simulations, and the sample state trajectories of the open-loop system and the closed-loop system are provided

in Figures 1–6 and Figures 7–12, respectively, where $x_i$, $i = 1, \ldots, 6$, are the components of the vector $[x_1^T(t) \;\; x_2^T(t) \;\; x_3^T(t)]^T \in \mathbb{R}^6$.

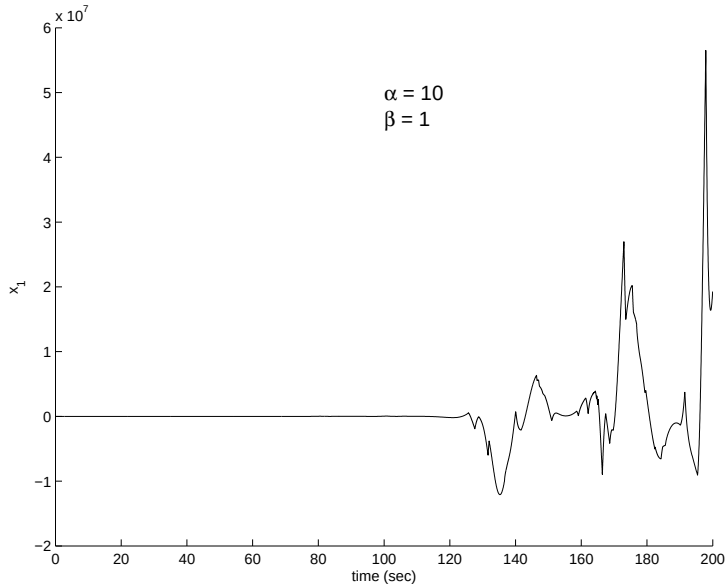


Fig. 1. Initial condition responses $x_1$ of the open-loop system.

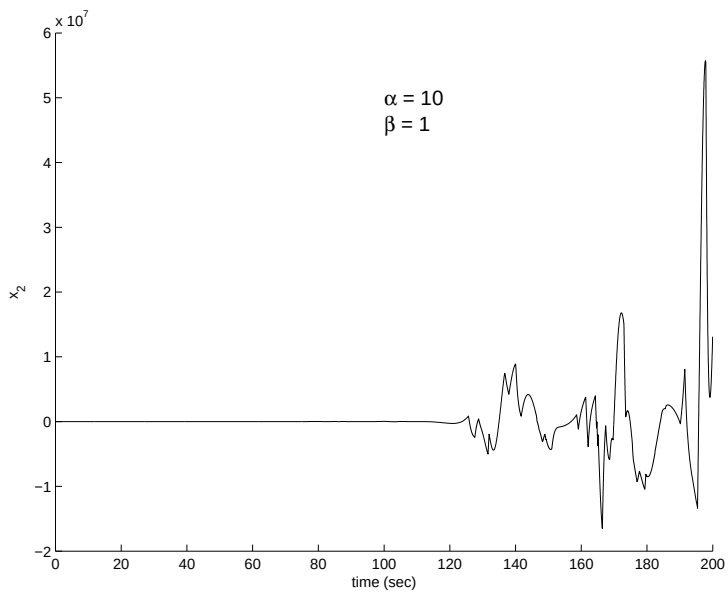


Fig. 2. Initial condition responses $x_2$ of the open-loop system.

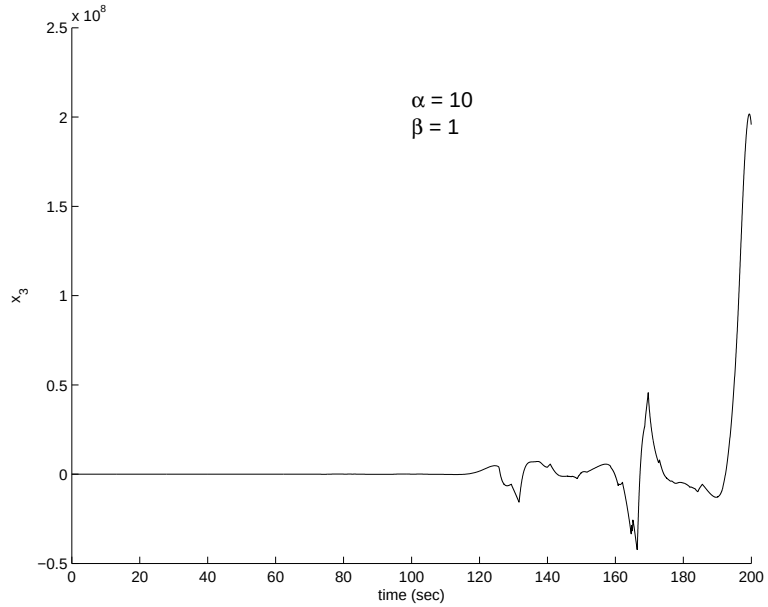


Fig. 3. Initial condition responses $x_3$ of the open-loop system.

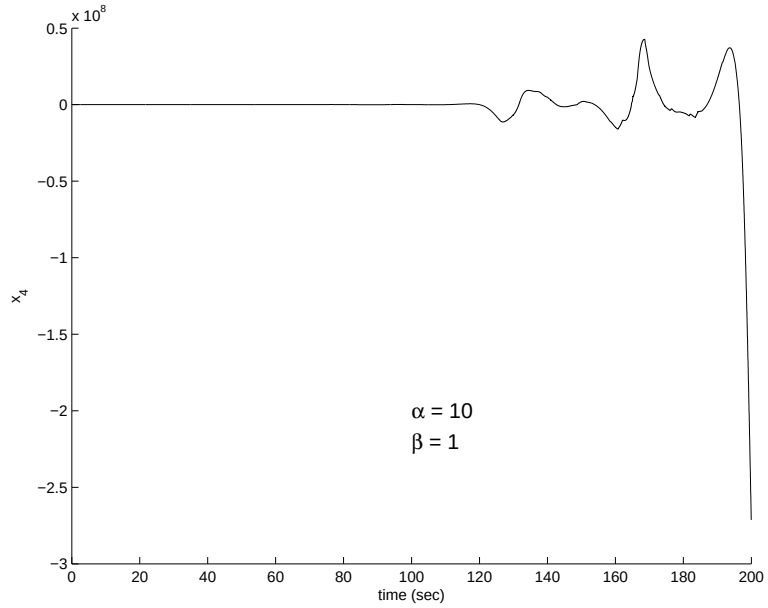


Fig. 4. Initial condition responses $x_4$ of the open-loop system.

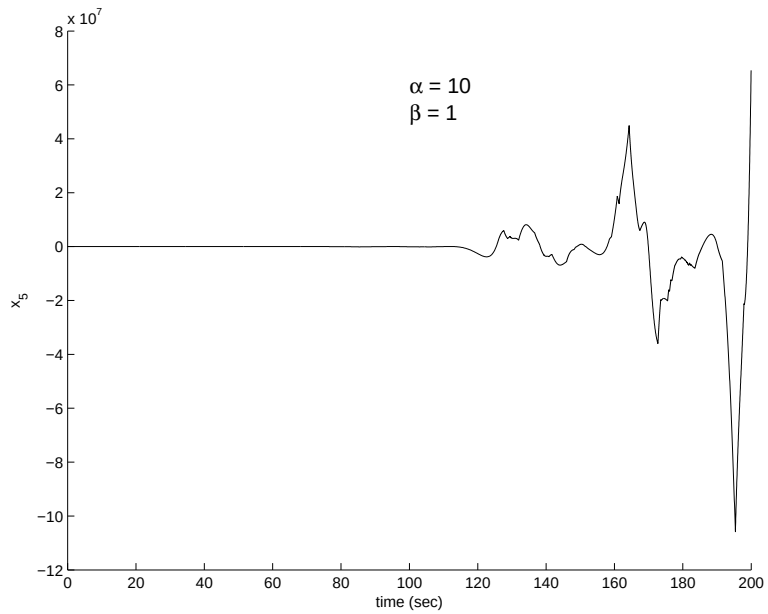


Fig. 5. Initial condition responses $x_5$ of the open-loop system.

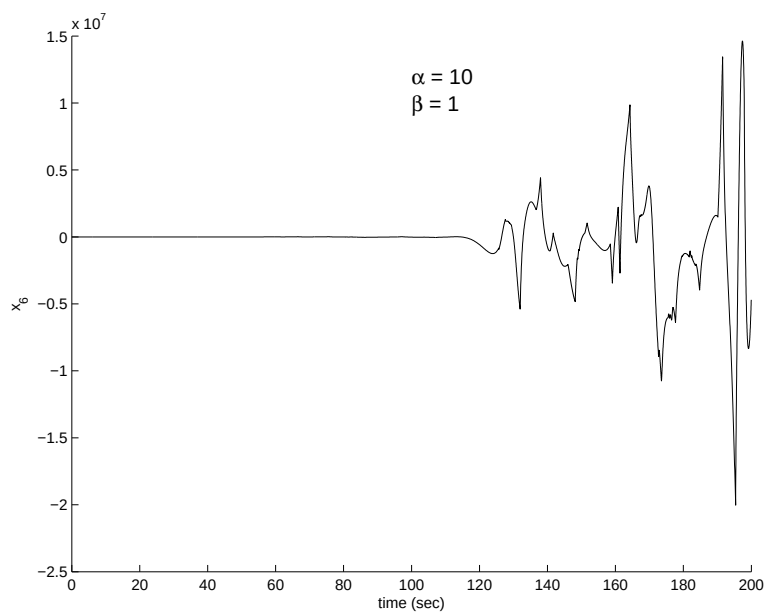


Fig. 6. Initial condition responses $x_6$ of the open-loop system.

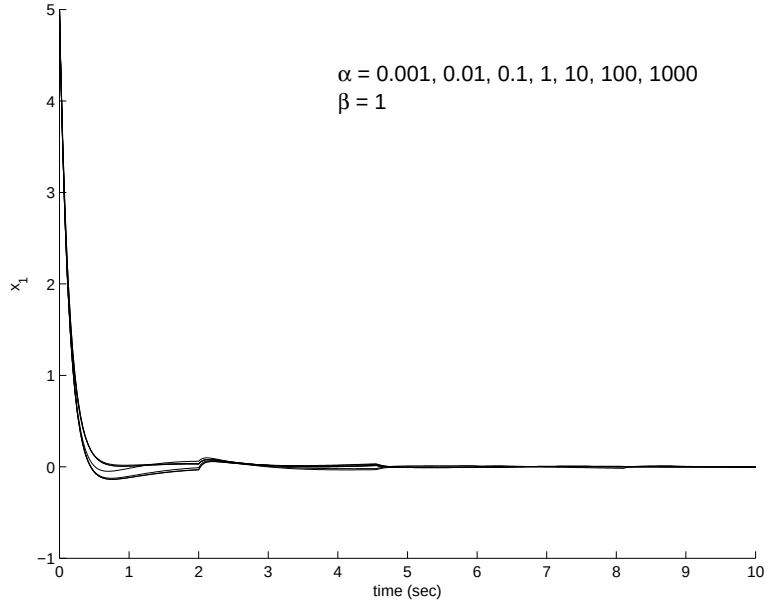


Fig. 7. Initial condition responses $x_1$ of the closed-loop system.

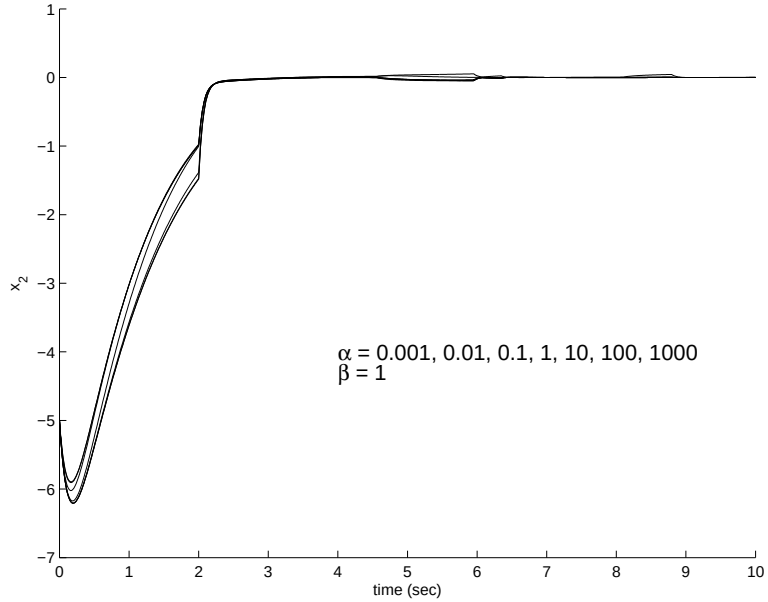


Fig. 8. Initial condition responses $x_2$ of the closed-loop system.

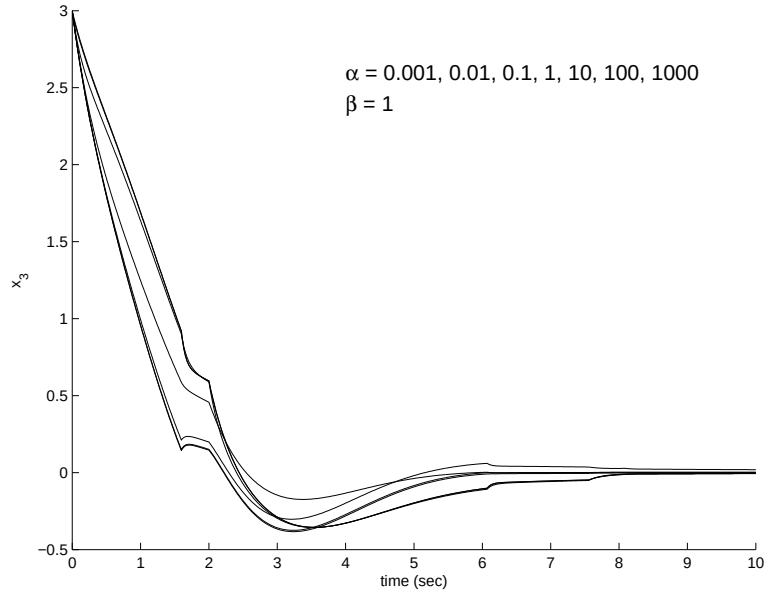


Fig. 9. Initial condition responses $x_3$ of the closed-loop system.

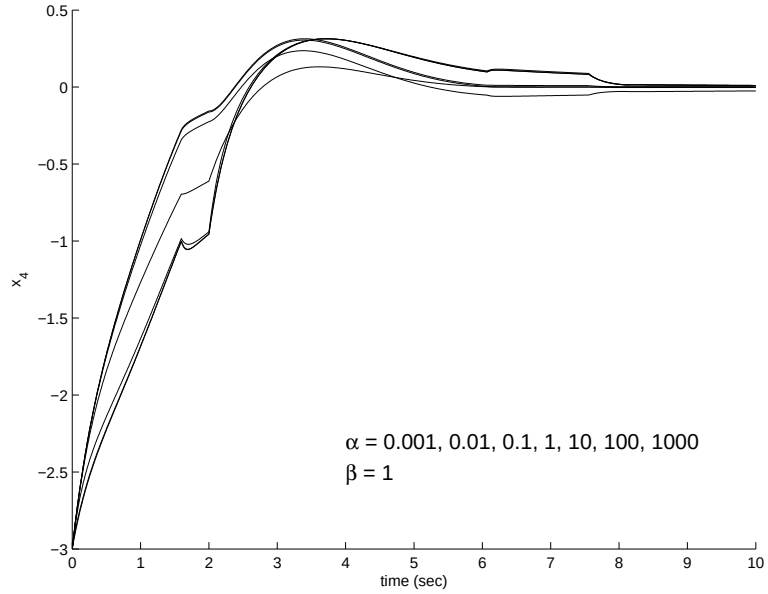


Fig. 10. Initial condition responses $x_4$ of the closed-loop system.

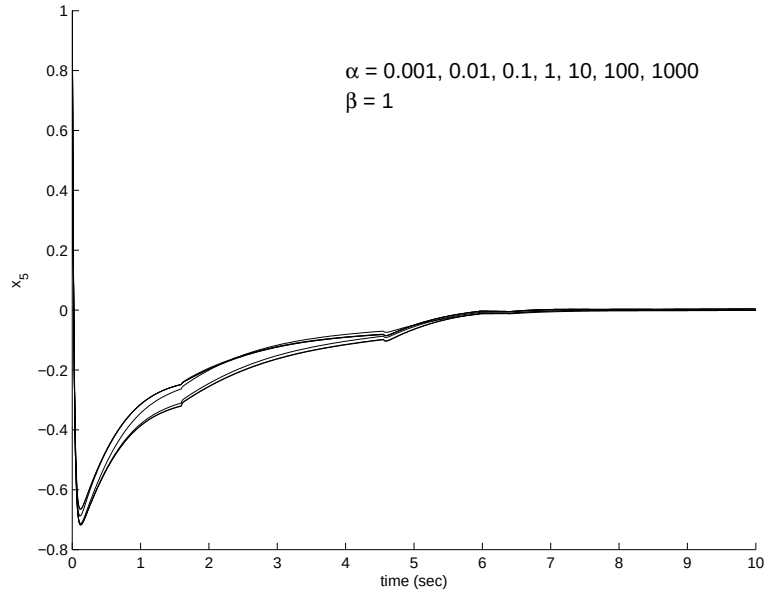


Fig. 11. Initial condition responses $x_5$ of the closed-loop system.

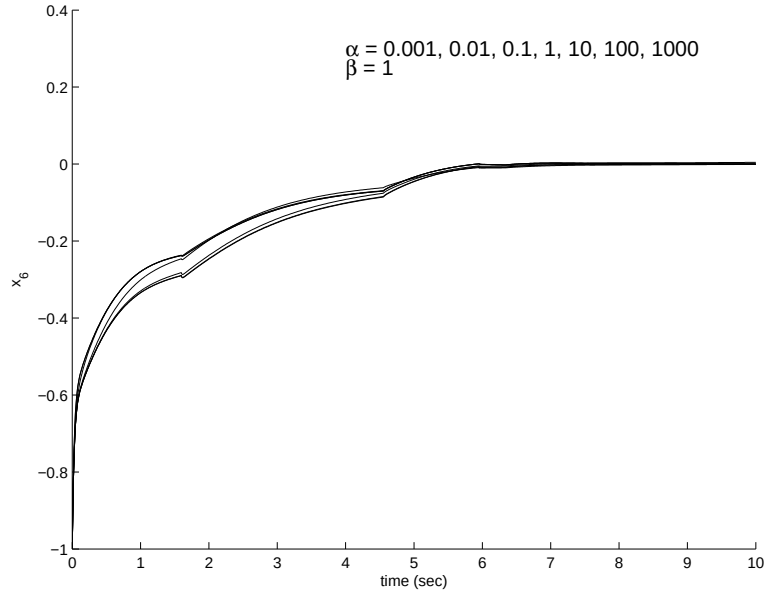


Fig. 12. Initial condition responses $x_6$ of the closed-loop system.